Fuel 182 (2016) 64–72

Contents lists available at ScienceDirect

Fuel

journal homepage: www.elsevier.com/locate/fuel

Full Length Article

Fe doping Pd/AC sorbent efficiently improving the Hg^0 removal from the coal-derived fuel gas

Lina Han [a], Xingxing He [a], Caixia Yue [b], Yongfeng Hu [c], Lina Li [d], Liping Chang [b], Hui Wang [b,*], Jiancheng Wang [b,*]

[a] College of Materials Science and Engineering, Taiyuan University of Technology, Taiyuan, China
[b] Key Laboratory of Coal Science and Technology, Ministry of Education and Shanxi Province, Taiyuan University of Technology, Taiyuan, China
[c] Canadian Light Source, 44 Innovation Boulevard, Saskatoon, SK, Canada
[d] Shanghai Synchrotron Radiation Facility, Shanghai Institute of Applied Physics, Chinese Academy of Sciences, Shanghai, China

GRAPHICAL ABSTRACT

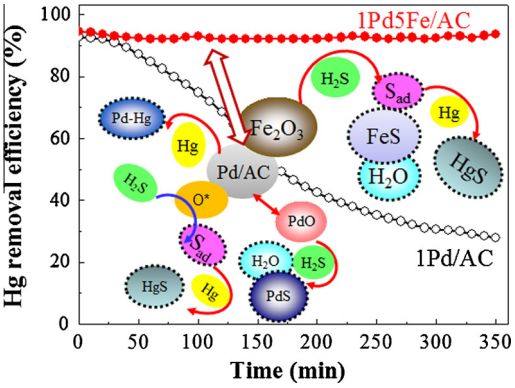

ARTICLE INFO

Article history:
Received 28 December 2015
Received in revised form 29 February 2016
Accepted 3 May 2016
Available online 24 May 2016

Keywords:
Hg^0 removal
Coal derived fuel gas
Fe doped Pd/AC sorbents

ABSTRACT

Fe doped Pd/AC (where AC is activated carbon) sorbents (1Pd5Fe/AC) were prepared and tested for removal of elemental mercury (Hg^0) from coal-derived fuel gas at medium range temperatures (150–250 °C). It is found that the Hg^0 removal efficiency of 1Pd5Fe/AC sorbent was much higher than that of 1Pd/AC sorbent, which has previously been shown to suffer from H_2S poisoning. 1Pd5Fe/AC sorbent can maintain its Hg^0 removal efficiency above 92% for 6 h at 200 °C. The fresh and used sorbents were characterized by X-ray diffraction (XRD), X-ray photoelectron spectroscopy (XPS) and X-ray absorption spectroscopy (XAS). The results indicated that the Hg^0 removal active components of the 1Pd5Fe/AC sorbent were elemental Pd and Fe_2O_3. The elemental Pd could react with mercury vapor to form Pd-Hg amalgam. Fe_2O_3 could react with H_2S to produce elemental sulfur which can combine with Hg^0 to form HgS. It is worth noting that PdO existed in both 1Pd5Fe/AC and 1Pd/AC sorbents and could react with H_2S to form PdS, which results in the deactivation of sorbents. But Fe_2O_3 on the surface of 1Pd5Fe/AC sorbent can compete with PdO to react with H_2S to produce elemental sulfur, thus inhibiting the deactivation of 1Pd5Fe/AC sorbent. In addition, H_2 and CO were found to promote the Hg^0 removal efficiency. The used 1Pd5Fe/AC sorbent could successfully be regenerated and reused for Hg^0 removal.

* Corresponding authors.
E-mail addresses: hui.wang@usask.ca (H. Wang), wangjiancheng@tyut.edu.cn (J. Wang).

http://dx.doi.org/10.1016/j.fuel.2016.05.046
0016-2361/

1. Introduction

Mercury, which is a highly toxic heavy metal, is considered a global threat to human health and environment. In 2013, the worldwide anthropogenic mercury emissions were estimated to be about 800 tons, whereas coal combustion contributed approximately 30% of this total [1]. In January 2013, world's first legally binding treaty on limiting the emissions and use of hazardous mercury (Minamata Convention on Mercury) was adopted by delegates from over 140 countries and regions [2].

Gasification has been one of the most efficient clean coal-conversion technologies and will continue to be widely used in future [3]. It has been reported that more Hg^0 and higher concentration of Hg^0 is emitted from coal gasification or pyrolysis than that from the coal combustion [4]. Additionally, due to its low solubility, Hg^0 is more difficult to be captured as compared to oxidized (Hg^{2+}) or particulate-bound mercury (Hg^p) [4–6]. Therefore, instead of capturing mercury from the combustion flue gas, mercury capture at higher temperature in gasification system is preferred in power generation. Thus, the removal of mercury at higher temperatures from coal derived fuel gas is essential for an efficient gas-cleaning of coal gasification systems due to the increased temperatures can maintain the overall thermal efficiency of a process [7].

The main goal of various mercury capture technologies is to oxidize Hg^0 to Hg^{2+} and then adsorb on the adsorbents. Reinhold Spörl and Rohan Stanger et al. [8–10] studied the capture of mercury on fly ash and the effect of oxygen-containing gas. But the mercury capture efficiency was low at high temperatures. Researchers also studied the Hg^0 oxidation on the surface of modified fly ash sorbents [11–13]. A homogeneous Hg^0 oxidation reaction mechanism with the released bromine species was proposed. It has been reported that activated carbon, particularly activated carbon impregnated with silver, sulfur and chlorine are effective for Hg^0 removal [14–17]. Some metal oxides and noble metals have been used for the Hg^0 removal from coal-derived fuel gas [18–20]. Pd/γ-Al_2O_3, Fe/γ-Al_2O_3 and PdFe/γ-Al_2O_3 sorbents prepared by our research group exhibited a good ability to remove Hg^0 from simulated coal gas. We found that there are two possible mechanisms for the capture of Hg^0 over the PdFe/γ-Al_2O_3 sorbent. One is either by the formation of HgS or by the formation of HgO and Pd–Hg amalgam [21]. We used two commercial iron oxide desulfurizers (TG-1 and TG-F) as sorbents to remove Hg^0. Due to its high content of Fe_2O_3, which is the main active component for Hg^0 removal, the Hg^0 absorption capacity of TG-1 was found to be higher than that of TG-F under the same operating conditions. The elemental sulfur, which was generated from the reaction of iron oxide with H_2S in TG-1 sorbent, can react with elemental mercury to form stable mercury sulfide, hence leading to an effective removal of Hg at low temperatures (140 and 160 °C) [22]. More recently, we prepared Pd/AC sorbent, which showed good performance for capturing Hg^0 from coal-derived fuel gas, while the effects of loading amount, reaction temperature, H_2 or O_2 pretreatments, and atmospheres were also systematically investigated [23,24].

Wu et al. have reported that Hg^0 can be removed from the coal-derived fuel gas containing H_2S with iron oxides (bulk and unsupported) at temperatures ranging from 60 °C to 100 °C. This is achieved when iron oxide first reacts with H_2S to form FeS_x and/or some surface elemental sulfur species, which then react with elemental mercury to form HgS [25–28]. A series of elemental mercury removal experiments and computational work results have been reported by Guo's group [29–31]. They considered that the significantly high Hg^0 removal efficiency of H_2S adsorbed Fe_2O_3 verifies the strong interaction between gaseous mercury and adsorbed sulfur species which is inferred in the theoretical study. Mercury compounds and new substances generated in the Fe_2O_3 samples after adsorbing H_2S and Hg^0 were detected as Hg^{2+}, sulfur, S^{2-}, S^- and Fe^{2+}. The Eley–Rideal mechanism, in which the adsorbed S_{ad} reacts with gas-phase Hg^0, has been proposed to explain the Hg^0 removal from coal gas by Fe_2O_3 [32].

In this paper, in order to suppress the deactivation of Pd/AC sorbent caused by H_2S and to further reduce the usage of Pd (hence more cost-savings), Fe was added to the 1Pd/AC sorbent, labeled as 1Pd5Fe/AC sorbent. The Hg^0 removal efficiency of the sorbents was conducted in the temperature range of 150–250 °C. The effects of H_2 and CO on the Hg^0 removal and the performance of the sorbent after regeneration were also studied. The fresh and used sorbents were characterized by XRD, XPS and XAS for interpreting the effect of Fe addition. The mechanism of Hg^0 removal over 1Pd5Fe/AC sorbent has also been discussed.

2. Experimental

2.1. Sorbent preparation

The commercially available (Shanxi Xinhua Chemical Co., Ltd., China) coal-based activated carbon (AC) with a diameter of 0.250–0.425 mm was selected as the sorbent support. Palladium nitrate and iron nitrate were used as precursors. After the impregnation, the sorbents were placed in air for 10 h. These were dried at 120 °C for 12 h and then were calcined in nitrogen at 500 °C for 5 h. Based on our previous work [23], the Pd/AC sorbent with 1.0 wt% Pd has showed high Hg^0 removal efficiency. Therefore, 1Pd/AC sorbent with 1.0 wt% Pd was prepared and then 5.0 wt% Fe_2O_3 was impregnated on the as-prepared 1Pd/AC sorbent to obtain 1Pd5Fe/AC sorbent.

2.2. Sorbent evaluation

The adsorption test was carried out using a fixed-bed quartz flow reactor at atmospheric pressure. The schematic diagram of experimental system was shown in our previous publication [21]. The apparatus consisted of a mercury vapor generating device, gas mixture system, fixed bed reactor, and an online mercury analyzer (Lumex RA-915M+Zeeman, Russia). The mercury vapor generator consisted of a mercury permeation tube (Valco Instruments Company Inc., USA), which was placed in a water bath system at 40 °C. Mercury vapors were brought in the fixed-bed quartz reactor using ultra high purity N_2. The coal-derived fuel gas consisted of 10 vol% H_2 (where applicable), 20 vol% CO (where applicable), 100 ppm H_2S, 40 ± 3 μg/m^3 mercury vapor and carrier gas (N_2). The flow rate of each gas stream was accurately controlled by a mass flow controller (MFC). 0.50 g sorbents were loaded in the quartz reactor (5.0 mm inner diameter and 64 cm length). Subsequently, the coal-derived fuel gas was introduced into the reactor at the desired temperature. The sorbent was exposed to the gas stream at a flow rate of 1000 ml/min, where the space velocity was 6.4×10^4 h^{-1}. The mercury vapor and H_2S concentrations at the inlet and outlet of the reactor containing sorbents were detected using an online mercury analyzer and a gas chromatograph equipped with a flame photometry detector (FPD).

The Hg^0 and H_2S removal efficiency (η) is used to evaluate the performance of the sorbents. η is calculated according to Eq. (1).

$$\eta\ (\%) = \frac{C_0 - C_1}{C_0} \times 100\% \quad (1)$$

where C_0 and C_1 are the inlet and outlet Hg^0 and H_2S concentrations (μg/m^3) respectively.

Mercury content of the sorbent after evaluation experiment is defined as mercury capacity (*MC*) and it can be directly measured

by the pyrolysis accessories (PYRO-915+) of mercury analyzer. 10 mg samples in each run were weighed accurately and loaded in the quartz boat and were sent into the pyrolyzing furnace. All mercury species released as elemental mercury were determined by the mercury analyzer. Theoretical adsorption mercury capacity (MC_T) of the sorbents can be calculated by the curve of the Hg^0 removal efficiency. The formula used to calculate MC_T is given in Eq. (2).

$$MC_T\ (\mu g/g) = \sum \eta_i \frac{C_0 Q_i t_i}{G \times 1000} \quad (2)$$

where η_i is the mercury removal efficiency at t_i which is the adsorption time at the i reactive time (min). C_0 is the initial concentration ($\mu g/m^3$) of Hg^0 in the feed gas, Q_i is the flow rate of the coal-derived fuel gas while G is the weight of sorbent (g) in the reactor.

2.3. Sorbent regeneration

After the mercury removal test, the 1Pd5Fe/AC sorbents (0.5 g) were regenerated by heating at 450 °C in pure N_2 (carrier gas) for 2 h and the Hg concentrations in outlet gas also were measured by the mercury analyzer. The regenerated sorbents were conducted under the same evaluation method (2.2) for Hg^0 removal. Mercury capacity (MC) of the regenerated sorbent after each evaluation was also detected by the pyrolysis accessories of mercury analyzer.

2.4. Sample characterization

Pore structure of samples was measured by nitrogen adsorption at −196 °C using a Micromeritics Tristar 3000 analyzer (Micromeritics. Ltd., USA). The specific surface area was calculated on the basis of the Brunauer–Emmett–Teller (BET) method. The pore size distribution was characterized by using the desorption branches of the N_2 adsorption isotherm and the Barrett–Joyner–Halenda (BJH) formula.

X-ray diffraction (XRD) was employed to investigate the crystal structure of the sorbents. The instrument used was a Rigaku D/max2500 diffractometer (Rigaku, Japan), fitted with a nickel-filtered Cu Kα radiation source operating at conditions of 40 kV and 100 mA. The scan rate was 8°/min with a range of 5–85°.

Surface analysis was conducted to determine the elemental speciation and concentration on the surface of the fresh and used sorbents, by using X-ray photoelectron spectroscopy (XPS). XPS analysis was conducted by using an ESCALAB 250 spectrometer (VG Scientific Ltd., UK) equipped with an Al Kα source (1486.6 eV, 150 W). Energy calibration was performed using the C 1s peak at 284.6 eV. No smoothing routine was applied to the data analysis.

X-ray absorption spectroscopy (XAS) spectra of Pd K-edge and Hg L-edge were collected using the XAFS beamline at the Shanghai Synchrotron Radiation Facility (SSRF), China. The SSRF electron storage ring was operated at 3.5 GeV with a beam operated in top-up mode. The source of the XAFS beam line is a single cycle Wiggler, delivering beam with $0.2 \times 0.3\ mm^2$ spot-size, 2×10^{-4} $\Delta E/E$ energy resolution, and a photon energy range of 3.5–50.0 keV. Spectral normalization and Fourier transform were performed using Athena. Sulfur K-edge XAS spectra were recorded using the Soft X-ray Micro characterization Beam line (SXRMB) of the Canadian Light Source, Canada, while the bulk sensitive fluorescence yield (FLY) was recorded using a micro-channel plate detector. The accuracy of the beam energy was 0.2 eV.

3. Results and discussion

3.1. Hg^0 removal efficiency over the sorbents

The Hg^0 and H_2S removal efficiencies of 1Pd/AC and 1Pd5Fe/AC sorbents were examined in N_2–Hg–H_2S atmospheres at temperatures of 150 °C, 200 °C and 250 °C. The results are shown in Fig. 1. It was found that within the initial 50 min, both 1Pd/AC and 1Pd5Fe/AC sorbents have similar Hg^0 removal efficiency. But the Hg^0 removal efficiency of 1Pd/AC sorbent significantly decreased in the range of 50 min to 350 min, while in the same time range, 1Pd5Fe/AC sorbent maintained its high and stable Hg^0 removal efficiency (more than 80% for 6 h at 150 °C and 200 °C). The Hg^0 removal efficiency of 1Pd5Fe/AC sorbent decreased to 67% when the temperature was 250 °C, while the Hg^0 removal efficiency of 1Pd/AC sorbent dropped even more, to 28% and 6% for corresponding temperatures of 200 °C and 250 °C respectively. These results showed that the addition of Fe can significantly improve the Hg^0 removal efficiency. Moreover, the high H_2S removal efficiency over the two sorbents can be obtained and a little better performance of the 1Pd5Fe/AC, which indicated that iron can improve the capturing H_2S.

Fig. 2 shows a comparison between the mercury capacities experimentally determined (MC) and theoretically calculated (MC_T) of 1Pd5Fe/AC sorbent. There was not much difference in both MC and MC_T of 1Pd5Fe/AC sorbent between 150 and 200 °C, but slightly decreased at 250 °C. These results were in accordance with the activity of the Hg^0 removal at different temperatures. MC and MC_T of 1Pd5Fe/AC sorbent at 150 °C were 22.3 and 25.8 μg/g respectively. The MC and MC_T values at the same temperature are slightly different. MC was measured by the pyrolysis accessories of mercury analyzer, which can detect all the mercury species on the used solid sorbents. MC_T was calculated by the curve of the Hg^0 removal efficiency obtained by the online mercury analyzer, which can only detect Hg^0 species in the gaseous phase. The difference in values between MC and MC_T should be the amount of the escaped mercury in oxidized state produced during the Hg^0 removal, except the errors in measurement and losses to the system. This difference was less than 4.5 μg/g and indicates that the escaped amount of the oxidized mercury was small and the main products were adsorbed on the sorbents.

Lee et al. summarized the previous studies on the mercury removal using carbon and fly ash with and without modification [33]. The results indicated that these sorbents only can be used at very low temperature (25–162 °C) although the adsorption capacity of the activated carbon with 3.5 wt% iodine is up to 3100–4800 μg/g. Li et al. [34] reported that the pyrolyzed tire showed a Hg^0 equilibrium adsorption capacity of approximately 406.5 μg/g at 120 °C. Liu et al. [35] studied of Hg^0 removal characteristics on Fe_2O_3 with H_2S and found that the high Hg^0 removal efficiencies were obtained at low temperature (⩽130 °C). The previous work of our group showed that at 200 °C, the 1Pd/γ-Al_2O_3 sorbent can operate for about 8 h with a Hg^0 removal efficiency of 84% in a Hg + N_2 atmosphere and it was decreased significantly as H_2S was added to the atmosphere. The efficiency of Hg^0 removal of the 1Pd5Fe/γ-Al_2O_3 sorbent is improved in Hg + N_2 + H_2S compared with 1Pd/γ-Al_2O_3 sorbent [21]. The Hg^0 removal efficiency of 1Pd/AC sorbent in N_2–H_2S–Hg–H_2 atmospheres can be maintained at about 91.4% for 360 min at 200 °C [24].

3.2. Effects of CO and H_2 on Hg^0 removal

CO and H_2 are the two main components of the coal-derived fuel gas. Therefore, it is necessary to study their effects on the Hg^0 removal. Hg^0 removal efficiencies of 1Pd/AC and 1Pd5Fe/AC

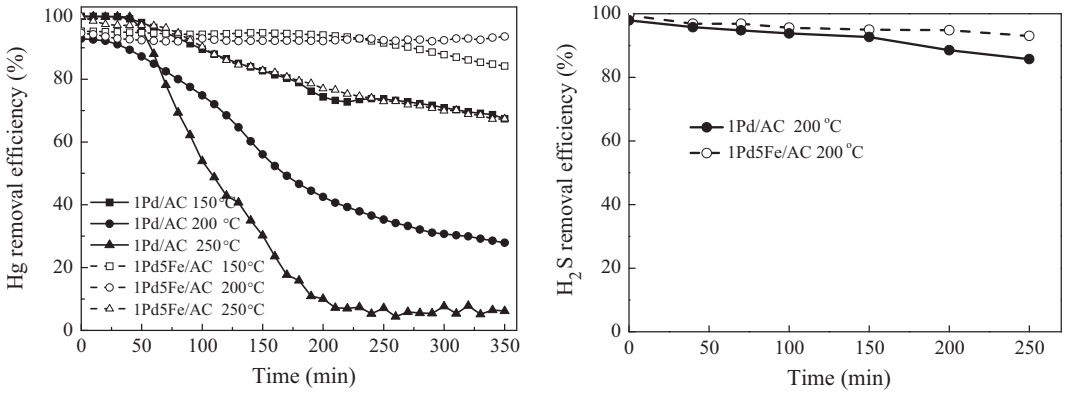

Fig. 1. Hg^0 and H_2S removal efficiency of 1Pd/AC and 1Pd5Fe/AC sorbents at different temperatures. (Reaction conditions: 40 μg/m^3 Hg^0 and 100 ppm H_2S in N_2, and SV = 6.4 × 10^4 h^{-1}.)

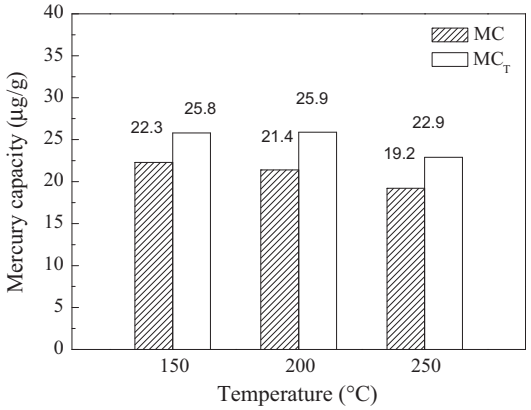

Fig. 2. Experimentally determined (MC) and theoretically calculated (MC_T) adsorption mercury capacity of sorbent 1Pd5Fe/AC at different temperature. (Reaction conditions: 40 μg/m^3 Hg^0 and 100 ppm H_2S in N_2, and SV = 6.4 × 10^4 h^{-1}.)

sorbents in N_2–H_2S–Hg and N_2–H_2S–Hg–H_2–CO atmospheres at 200 °C were compared. The results are shown in Fig. 3. It can be seen that the Hg^0 removal efficiencies of 1Pd/AC and 1Pd5Fe/AC sorbents in N_2–H_2S–Hg–H_2–CO atmosphere were much better than those in N_2–H_2S–Hg atmosphere. For 1Pd5Fe/AC sorbent, the Hg^0 removal efficiencies in the absence and presence of CO and H_2 maintained their values above 92% and 95% for 6 h respectively. For 1Pd/AC sorbent, the Hg^0 removal efficiencies (in presence or absence of CO and H_2) maintained their values at above 80% for 90 min and 240 min respectively. It can be concluded that a reducing atmosphere could improve the Hg^0 removal efficiency over both 1Pd/AC and 1Pd5Fe/AC sorbents. In addition, 1Pd/AC sorbent might suffer more serious H_2S toxic effect and therefore, the improvement of the Hg^0 removal efficiency for 1Pd/AC sorbent was more obvious than that for 1Pd5Fe/AC sorbent. Our previous study indicated that H_2 and CO can enhance the efficiency of the removal of Hg over the $PdO–Fe_2O_3/\gamma$-Al_2O_3 sorbent at 250 °C [21]. Zhou et al. [36] researched the elemental mercury removal from syngas by nano-ZnO. It is found that a promoting effect for Hg^0 removal efficiency of nano-ZnO was observed when H_2 and CO were introduced to mixture gas flow of N_2–Hg–H_2S.

3.3. Performance of the sorbents after regeneration

The used 1Pd5Fe/AC sorbents were regenerated by heating at 450 °C in pure N_2 (carrier gas) for 1 h. Then their ability to remove Hg^0 was tested at 200 °C. The results are shown in Fig. 4. It can be seen from Fig. 4 that after the primary recycling, the Hg^0 removal efficiency of 1Pd5Fe/AC sorbent decreased from 91.6% to 52.3% in 240 min. Interestingly, the Hg^0 removal efficiency after the subsequent recycling at 240 min improved somewhat [to 58.4% (after the second recycling) and 62.9% (after the third recycling)]. This suggested that some chemisorbed substance on the used 1Pd5Fe/AC sorbent could have decomposed to release active species for

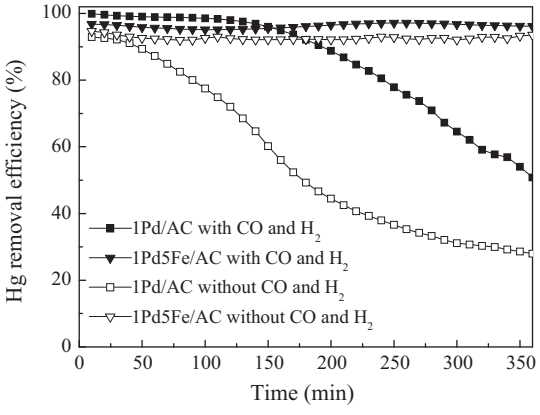

Fig. 3. Effects of CO and H_2 on the Hg^0 removal efficiencies of 1Pd/AC and 1Pd5Fe/AC sorbents. (Reaction conditions: 200 °C, 40 μg/m^3 Hg, 100 ppm H_2S, 20 vol% CO, 10 vol% H_2 in N_2, and SV = 6.4 × 10^4 h^{-1}.)

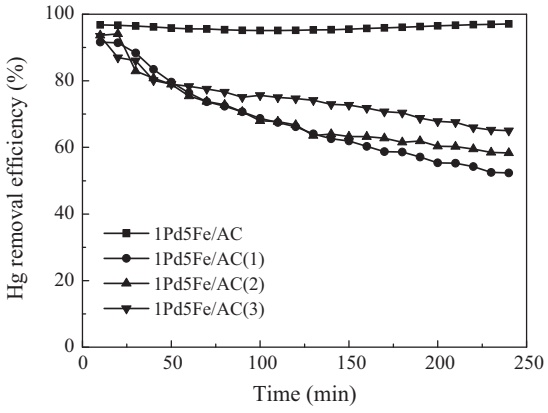

Fig. 4. Mercury removal efficiency of 1Pd5Fe/AC sorbent after several recycling (1Pd5Fe/AC: fresh sorbent; 1Pd5Fe/AC(1): sorbent after primary recycling; 1Pd5Fe/AC(2): sorbent after secondary recycling; 1Pd5Fe/AC(3): sorbent after tertiary recycling).

Hg^0 removal. Part of the active substance in the pore structure of the support (i.e. activated carbon) could gradually move to the surface of sorbent and take part in the reactions of Hg^0 removal. Comparing the results of regeneration of 1Pd/AC reported by our previous work [24] and 1Pd5Fe/AC sorbents, the variation trend of the Hg^0 removal efficiencies of these two sorbents after recycling were similar, but the Hg^0 removal efficiency of 1Pd5Fe/AC sorbent before and after regeneration was superior to that of 1Pd/AC sorbent.

The mercury capacity and Hg desorption amount of each regeneration was given in Table 3, the mercury capacity and Hg desorption amount decreased when the sorbent was subjected the first and second regeneration. Almost all the Hg can be released from the 1Pd5Fe/AC sorbent because the mercury capacity, 12.2 μg/g (1st regeneration) with Hg desorption amount, 12.8 μg/g (1st desorption) almost the same, which indicated that the Hg containing in the used sorbent can be easily regenerated.

3.4. Analysis of the fresh and used sorbents

3.4.1. BET analyses of sorbents

The physical properties of AC support, 1Pd/AC and 1Pd5Fe/AC sorbents including BET surface area, pore volume and pore diameters are summarized in Table 1. The support (AC) and the 1Pd/AC catalyst had almost the same surface characteristics. However, their BET surface area measurements suggested that adding Fe_2O_3 reduced the surface area and pore volume. It might be due to the reason that the 1Pd5Fe/AC sorbent was prepared by impregnating 5.0 wt% Fe_2O_3 on the as-prepared 1Pd/AC sorbent. It means that twice calcinations at 500 °C resulted in the sintering of the pore structure. Although 1Pd5Fe/AC sorbent had a lower BET surface area, its ability to remove Hg^0 was better than that of 1Pd/AC sorbent. Therefore, the differences of the pore structure between the 1Pd5Fe/AC and 1Pd/AC sorbents should not the main reasons for the different Hg^0 removal efficiencies.

3.4.2. XRD analyses of sorbents

The results of XRD analysis of the fresh and used 1Pd/AC and 1Pd5Fe/AC sorbents are shown in Fig. 5. No obvious diffraction peaks of Fe_2O_3 are detected in both fresh and used 1Pd5Fe/AC sorbents. It is possible that Fe_2O_3 existed as amorphous and/or in uniform distribution. The diffraction peaks of elemental Pd were found at 40.1° and 67.8° over the fresh 1Pd/AC and 1Pd5Fe/AC sorbents respectively [37]. The other Pd diffraction peaks at 26.9°, 36.0° and 43.5° are mainly obscured by the AC support. The elemental Pd was one of the main palladium species in the fresh 1Pd/AC and 1Pd5Fe/AC sorbents. The characteristic peaks of elemental Pd at 40.1° and 67.8° could no longer be observed for the used 1Pd/AC and 1Pd5Fe/AC sorbents. It suggested that the elemental Pd is the active species for removing Hg^0 over Pd/AC and 1Pd5Fe/AC sorbents. The characteristic peaks of Hg product are not resolved in XRD. In order to study the chemical states of the fresh and used 1Pd/AC and 1Pd5Fe/AC sorbents, XPS and XAS techniques were used. The results of the analyses have been shown in Fig. 5.

Table 1
Physical properties of support and sorbents before and after Fe doped.

Samples	BET surface area (m^2/g)	Pore volume (cm^3/g)	Average pore diameter (nm)
AC	915.56	0.51	2.39
1Pd/AC	926.48	0.52	2.44
1Pd5Fe/AC	774.43	0.44	2.35

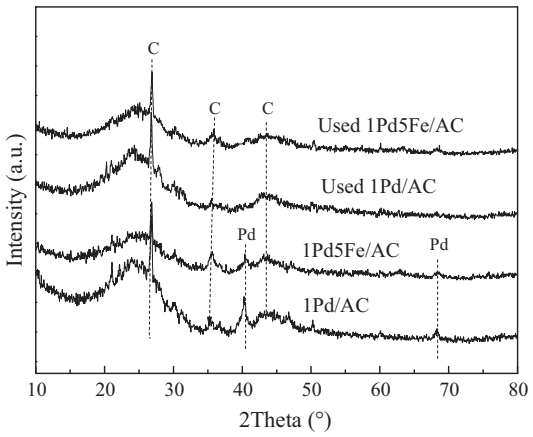

Fig. 5. XRD patterns of fresh and used 1Pd/AC and 1Pd5Fe/AC sorbents.

3.4.3. XPS analyses of sorbents

The Pd 3*d* XPS spectra of 1Pd/AC and 1Pd5Fe/AC sorbents before and after the Hg^0 adsorption are shown in Fig. 6. The peak intensity of XPS spectra reflects the content of atoms at the surface [37]. Gaussian–Lorentzian profiles were used to fit Pd and S. The subsequent results have been presented in Table 2. It can be seen from Fig. 6a that the binding energies (BEs) of Pd $3d_{5/2}$ at 335.5 eV and those of Pd $3d_{3/2}$ at 340.9 eV could be assigned to Pd^0 [38]. The BEs of Pd 3*d* at 337.0 eV and 342.3 eV were in good agreement with the data of PdO given in reference [39,40]. It can also be observed that the Pd^0/Pd ratios of the fresh 1Pd/AC and 1Pd5Fe/AC sorbents were 68% and 58% respectively. These results indicated that the main Pd species on the surfaces of the fresh sorbents was Pd^0 as well as a small quantity of PdO. Due to the effect of Fe_2O_3, there was a slight shift in the Pd 3*d* binding energies of the fresh 1Pd5Fe/AC sorbent compared to the 1Pd/AC sorbent. As can be seen in Table 2, the Pd content of 1Pd5Fe/AC (0.18 wt%) was much lower than that of 1Pd/AC sorbent (0.44 wt%) due to the surface modification by Fe_2O_3.

After the capture of Hg^0, Pd^0 and Pd^{2+} peaks can also be observed in the XPS spectra of the used 1Pd/AC and 1Pd5Fe/AC sorbents (Fig. 6b). But Pd^{2+} peak is shifted lower to 336.5 eV. This is more likely due to the formation of PdS in the used sorbent ($H_2S_{(g)} + PdO \rightarrow PdS + H_2O$). The BE of Pd $3d_{5/2}$ of PdS has been reported to be 335.8–336.9 eV [33,41,42]. All of these were less than 337.0 eV (the BE of PdO), thus indicating that the Pd species on the surfaces of the used 1Pd/AC and 1Pd5Fe/AC sorbents were Pd^0, PdO and PdS. The Pd^0/Pd ratios of the used 1Pd/AC and 1Pd5Fe/AC sorbents were 24% and 16% respectively. It means that the Pd^{2+} species was dominantly present on the used sorbents. The results suggested that Pd^0 was oxidized by the adsorbed oxygen or the oxygen-containing functional group (such as –COO– and –CO) on the AC surface to PdO, and later reacted with H_2S to produce PdS during the Hg^0 removal.

Fig. 7 presents the XPS spectra of Fe 2*p* of the fresh and used 1Pd5Fe/AC sorbents and those of S 2*p* of the used 1Pd/AC and 1Pd5Fe/AC sorbents. The photoelectron peaks at the center of 710.8 eV and 724.5 eV in the fresh and used 1Pd5Fe/AC sorbents can be assigned to the mixture of Fe $2p_{3/2}$ and $2p_{1/2}$ peaks of Fe^{2+} and Fe^{3+} [35,43]. Azhar Uddin's group [25,27] studied the iron oxide sorbents for Hg^0 removal from coal gas and suggested that the reduction of iron oxide with H_2 and CO according could be occurred under some conditions. So, the reduction of Fe_2O_3 to Fe_3O_4 over PdFe/AC should be occurred. Tan et al. [18] studied the removal of elemental mercury in flue gas using Fe_2O_3–SiO_2 sorbent. It is found that the adsorbed Hg^0 would react with lattice oxygen provided by the Fe_2O_3, while the intermediate product

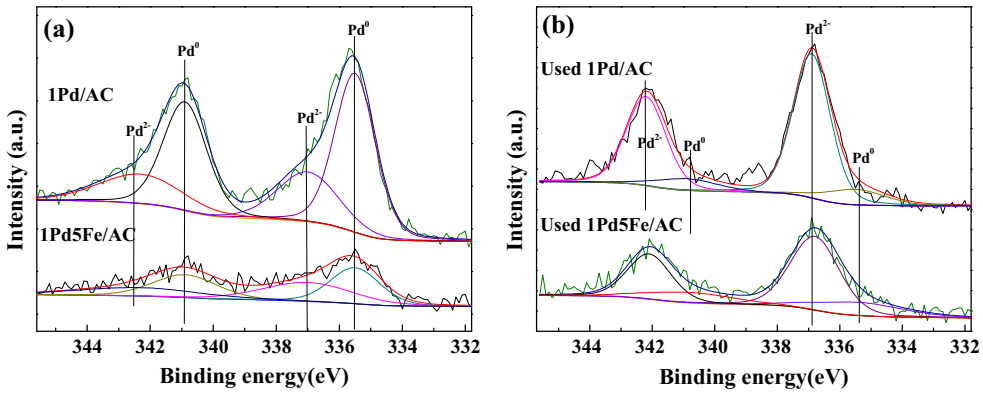

Fig. 6. XPS spectra of Pd 3*d* on the surface of (a) fresh and (b) used 1Pd/AC and 1Pd5Fe/AC sorbents.

Table 2
Contents of Pd, S and Fe on the surface fresh and used sorbents from XPS spectra.[a]

Samples	Fe (wt%)	Pd (wt%)	Pd^0/Pd (%)	S (wt%)	S^{2-}/S (%)
1Pd/AC	–	0.44	68	–	–
1Pd5Fe/AC	2.25	0.18	58	–	–
Used 1Pd/AC	–	0.24	24	1.78	30[b]
Used 1Pd5Fe/AC	2.08	0.20	16	1.92	40

[a] Gaussian–Lorentzian method (Gaussian/Lorentzian: 20%) was used, the ratio area between Pd3d5/2 and Pd3d3/2 is fixed at 3:2.
[b] The data of S^{2-} were governed by PdS and FeS.

Table 3
Mercury capacity and Hg desorption amount of the regeneration.

	Mercury capacity MC (μg/g)	Hg desorption amount (μg/g)[a]
Fresh 1Pd5Fe/AC	13.1	12.8
1st regeneration	12.2	11.8
2nd regeneration	10.5	10.5
3rd regeneration	10.3	

[a] According to Hg desorption curve.

could be Fe_3O_4 or FeO. The Fe $2p_{1/2}$ peak for FeS and Fe^{3+}–S/Fe^{2+}–S has been reported at 711.05 and 710.9 eV [44,45]. So Fe^{2+} species on the surface of the used 1Pd5Fe/AC sorbent could be FeS. It has been reported that Fe_2O_3 can react with H_2S to produce FeS and elemental sulfur ($Fe_2O_3 + 3H_2S \rightarrow 2FeS + S_{ad} + 3H_2O$) [21].

From S 2*p* XPS spectra of the AC support and the used 1Pd/AC and 1Pd5Fe/AC sorbents shown in Fig. 7b, it can be seen that the peak at 164.5 eV of S 2*p* of the used 1Pd/AC and 1Pd5Fe/AC sorbents was assigned to elemental S. The 162.6 eV peak of the used 1Pd/AC sorbent and 1Pd5Fe/AC was assigned to PdS [46]. The S 2*p* peak at 163.3 eV of the used 1Pd5Fe/AC sorbent was assigned to S_n^{2-} [47], which is in agreement with the results of Fe 2*p*. It is found that the S content of the used 1Pd/AC and 1Pd5Fe/AC sorbents were 1.78 wt% and 1.92 wt% respectively, while the S^{2-}/S ratios of the used 1Pd/AC and 1Pd5Fe/AC sorbents were 30% and 40% (see Table 2) respectively. The different ratios of S^{2-}/S suggested that Fe_2O_3 in the 1Pd5Fe/AC sorbent can react with H_2S to form FeS_x. Considering that H_2S could react with PdO in 1Pd/AC and 1Pd5Fe/AC sorbents to produce PdS, the reaction of Fe_2O_3 and H_2S could hinder the reaction between PdO and H_2S to improve the efficiency of the Hg^0 removal.

3.4.4. XAS analyses of sorbents

Pd K-edge, S K-edge, and Hg L-edge XAS were studied for both fresh and used sorbents. In order to further reveal the bonding environment of Pd, such as the bond distance and the coordination number, the extended X-ray absorption fine structure spectra of above sorbents via the Fourier transform were also carried out.

Fig. 8a shows the Pd K-edge EXAFS results of fresh and used sorbents and those of the reference samples plotted in R space. For fresh 1Pd/AC sorbent, a dominant peak at about 2.538 Å (all bond distances are without phase correction) corresponds to the first shell Pd–Pd bonding. This was different from those of the Pd foil and the fresh 1Pd5Fe/AC sorbent. It is found that the R space results of all used sorbents were similar and the bond lengths were between those of the Pd–O and Pd–Pd (Fig. 8a). So it can be deduced that Pd in the used 1Pd/AC was in the form of PdS, which

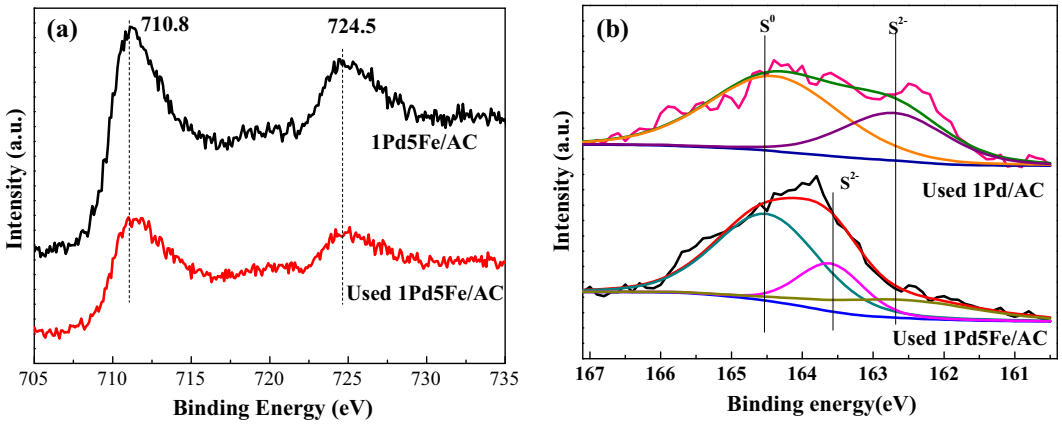

Fig. 7. XPS spectra of (a) Fe 2*p* and (b) S 2*p* on the surface of sorbents.

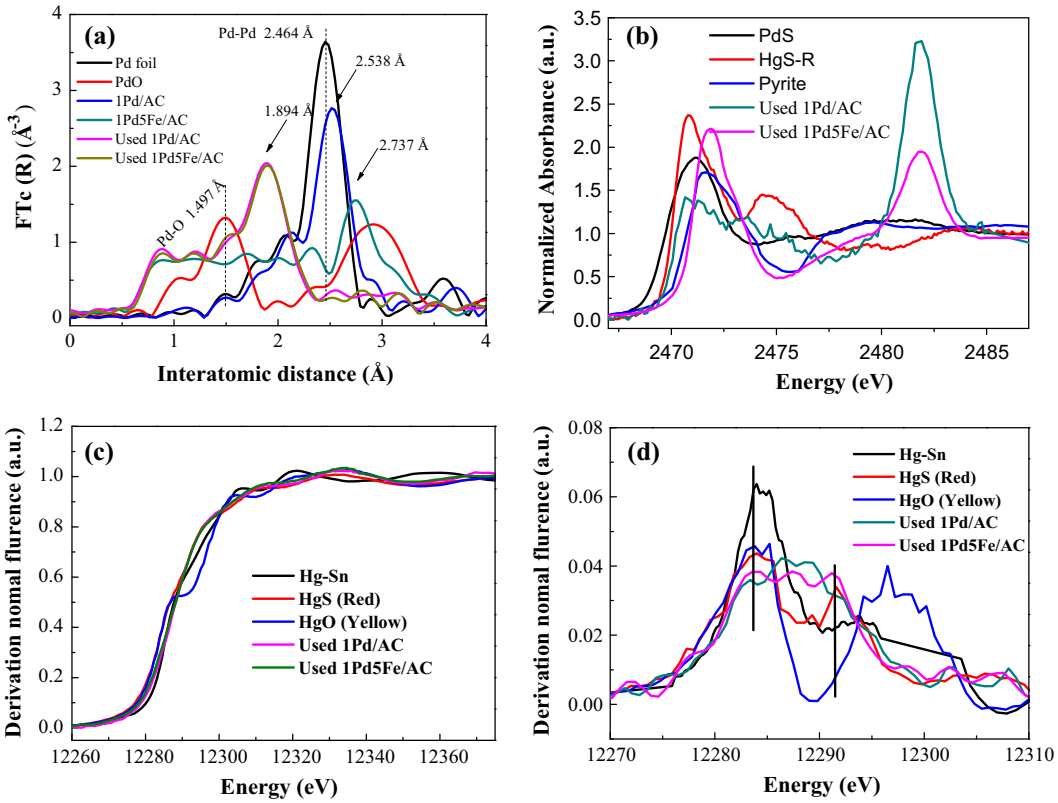

Fig. 8. XAS spectra of fresh and used sorbents and reference samples: (a) Pd K-edge EXAFS Fourier transform spectra, (b) S K-edge, (c) Hg L3-edge, and (d) the first derivative of the spectra.

was in agreement with the Pd 3*d* and S 2*p* results of the used 1Pd/AC [7,24]. However, for the used 1Pd5Fe/AC sorbent, there was some PdO or PdS due to the change of the electronic environment after Fe addition.

The S K-edge XANES spectra of the used 1Pd/AC and 1Pd5Fe/AC sorbents and those of the reference samples are shown in Fig. 8b. It can be observed that the energy of the main peak of S gradually increases from about 2470.8 eV to 2481.8 eV with the increase of oxidation number from −2 to +6. The main peaks of red HgS, PdS and pyrite were observed at 2470.8 eV, 2471.1 eV and 2471.4 eV respectively. According to the results obtained in one of our previous studies, sulfate and organic sulfur could be found on the AC support [48]. For the used 1Pd/AC sorbent, the broad peak around 2471.1 eV should be assigned to the reduced sulfur species, such as the mixtures of PdS, HgS, elemental S and other sulfur from the AC support. However, the first peak of the used 1Pd5Fe/AC sorbents at 2471.9 eV can mainly be attributed to FeS_x such as pyrite. The peak at 2481.8 eV of the used 1Pd/AC and 1Pd5Fe/AC sorbents should come either from sulfate sulfur in the AC support or from the oxidized surface sulfur of the sorbents. The formation of different S species between the 1Pd/AC and 1Pd5Fe/AC sorbents could be the key point to interpret the difference in their Hg^0 removal performances. This is due to the reason that PdO on the surface of 1Pd/AC sorbent could react with H_2S to produce PdS, which enhances the Pd → PdO transition, resulting in the decrease of the available Pd for the Hg^0 removal. On the other hand, Fe_2O_3 can consume part of H_2S thus preventing H_2S from reacting with Pd and maintaining the high Hg^0 removal ability for the 1Pd5Fe/AC sorbent.

Fig. 8c and d shows the Hg L_3-edge XANES spectra and their corresponding first order derivative spectra of the used sorbents and reference samples. Instead of Hg–Pd amalgam reference compounds, Hg–Sn amalgam, together with yellow HgO and red HgS were chosen as the Hg reference compounds. It can be seen from Fig. 8 that the energy positions of two used sorbents fall in between those of Hg–Sn amalgam and HgS. There was only one peak in first order derivative spectrum of Hg–Sn alloy. There were two obvious peaks which belonged to the transition of 6*s* and 6*p* orbital in the Hg L_3-edge first order derivative XANES spectrum of HgO and HgS, while the distances between the two peaks were about 13.3 eV and 7.5 eV respectively [49]. It can be seen from Fig. 8d that the first order derivative spectra of the Hg L_3-edge spectrum of the used 1Pd/AC and 1Pd5Fe/AC sorbents were between that of the Hg-Sn alloy and HgS. In comparison to the used 1Pd/AC and 1Pd5Fe/AC sorbents, HgO had a very different near edge spectrum. The splitting in the derivative spectrum of HgO was too large. These results indicated that the Hg^0 being captured is certainly not in the form of HgO, rather is most likely a mixture of Pd–Hg amalgam and HgS. Previous studies [23,24,50] have reported that Pd as an active metal can efficiently be captured at high temperature (200–350 °C), and that the elemental S can efficiently absorb Hg only at low temperature (usually lower than 150 °C). It should be noted that the amount of Hg products in the sorbents is only 20 ug/g. Therefore, no attempt was made to distinguish the Pd-Hg amalgam and HgS amounts based on our Hg L_3-edge XANES results.

3.5. Discussion of mechanism

3.5.1. Mechanism of the Hg^0 removal

In this study, according to the characteristic results, different performances of the sorbents can now be discussed in details. The ratio of Pd^0/Pd on the surface of the fresh 1Pd/AC sorbent was 68% (as shown in Table 2) with the rest of Pd being in the form of PdO. So, the active component for Hg^0 removal on 1Pd/AC sorbent was mainly elemental Pd. The elemental Pd could react with mercury vapor to form Pd–Hg amalgam for 1Pd/AC sorbent [50],

which was the main reaction for the Hg^0 removal from coal-derided fuel gas on the 1Pd/AC sorbent. However, PdO could react with H_2S to form PdS [51]. The formation of PdS can lead to the consumption of PdO, which induced the Pd → PdO transition, resulting in a decrease in available Pd for the Hg^0 removal. It can be deduced that the deactivation of 1Pd/AC sorbent could be due to the generation of PdS. In addition, the XPS results indicated the existence of the elemental S, which should come from H_2S. Guo et al. [29] considered that the Eley–Rideal mechanism with Hg^0 adsorption on H_2S/α-Fe_2O_3 surface was the only possible mechanism of the reaction process, where H_2S is firstly dissociated in two steps, i.e., $H_2S \rightarrow HS + H$ and $HS \rightarrow S + H$ by the catalytic effect of α-Fe_2O_3. The adsorbed sulfur reacts with gaseous Hg^0 to form HgS. H_2S could be oxidized on the 1Pd/AC sorbent. The elemental S could react with Hg^0 to generate HgS [22,25], which was another path for the Hg^0 removal. However, the elemental S can be volatile at higher temperatures, due to which, the formation of HgS could only occur at lower temperatures (<200 °C) [11]. In N_2–H_2S–Hg system, for 1Pd/AC sorbent, the corresponding reaction equations for Hg^0 removal from coal-derived fuel gases can be represented by Eqs. (a1)–(a4).

$$Hg^0 + Pd^0 \rightarrow Hg - Pd \quad (a1)$$

$$H_2S_{(g)} + PdO \rightarrow PdS + H_2O \quad (a2)$$

$$H_2S_{(g)} + O^* \rightarrow S_{ad} + H_2O \quad (a3)$$

$$S_{ad} + Hg^0 \rightarrow HgS \quad (a4)$$

where S_{ad} is active surface sulfur, and O^* denotes the surface oxygen and the lattice oxygen in metal oxides on the sorbents.

The active components of the 1Pd5Fe/AC sorbent were elemental Pd and Fe_2O_3. The reactions of Pd on the 1Pd5Fe/AC sorbent were the same as those on 1Pd/AC sorbent. On the other hand, Fe_2O_3 can react with H_2S to produce elemental sulfur ($Fe_2O_3 + 3H_2S \rightarrow 2FeS + S_{ad} + 3H_2O$) which can combine with Hg^0 to form HgS. These reactions can alleviate the reaction between PdO and H_2S because the amount of Fe_2O_3 is far more than that of PdO. It was inferred that abundant Fe_2O_3 could inhibit the deactivation of 1Pd5Fe/AC sorbent due to the formation of PdS. For 1Pd5Fe/AC sorbent, the corresponding reaction equations for Hg^0 removal from coal-derived fuel gas are given by Eqs. (b1)–(b5).

$$Hg^0 + Pd^0 \rightarrow Hg - Pd \quad (b1)$$

$$H_2S_{(g)} + O^* \rightarrow S_{ad} + H_2O \quad (b2)$$

$$S_{ad} + Hg^0 \rightarrow HgS \quad (b3)$$

$$H_2S_{(g)} + PdO \rightarrow PdS + H_2O \quad (b4)$$

$$3H_2S_{(g)} + Fe_2O_3 \rightarrow 2FeS + S_{ad} + 3H_2O \quad (b5)$$

All the reactions given by Eqs. (b1)–(b5) on the surface of 1Pd5Fe/AC sorbent have been summarized in Fig. 9. When there was 10 vol% H_2 and 20 vol% CO in the atmosphere, PdO could easily be reduced to Pd^0 ($PdO \rightarrow Pd^0$), which can then react with Hg^0 to produce Hg–Pd amalgam. At the same time, the reaction between PdO and H_2S was suppressed due to the reduction of PdO. Therefore, the Hg^0 removal efficiencies in atmospheres with H_2 and CO were higher than those without H_2 and CO.

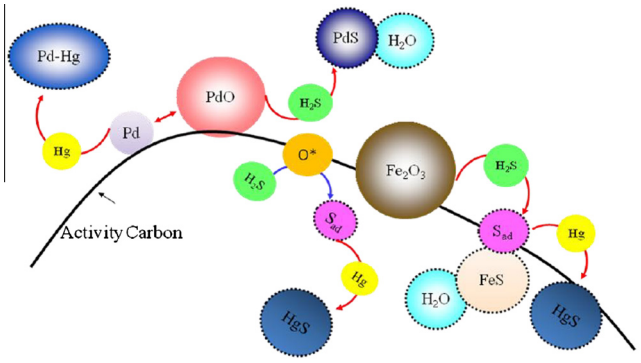

Fig. 9. Possible reactions on the surface of 1Pd5Fe/AC sorbent.

3.5.2. Mechanism of sorbent deactivation

It can be seen from Table 2 that the ratios of Pd^0/Pd on the surface of fresh 1Pd/AC and 1Pd5Fe/AC sorbents were 68% and 58% respectively. The rest of Pd should be PdO. There was a transition between Pd^0 and PdO ($Pd^0 \leftrightarrow PdO$) during the process of Hg^0 removal. Although the ratios of PdO/Pd on the surfaces of the fresh 1Pd/AC and 1Pd5Fe/AC sorbents were low, yet PdO can play an important role. PdO could react with H_2S to form PdS. The reaction can be represented by Eq. (c1).

$$H_2S_{(g)} + PdO \rightarrow PdS + H_2O \quad (c1)$$

PbO was consumed by the reaction with H_2S. Thus, the transition of $Pd^0 \rightarrow PdO$ was enhanced. It resulted in the decrease of available Pd for the Hg^0 removal. At last, the sorbents would lose their ability of Hg^0 removal. It can be expressed by reaction equation (c2).

$$Pd \leftrightarrow PdO \rightarrow PdS \quad (c2)$$

The ability to remove Hg^0 for the 1Pd5Fe/AC sorbent was better than that of the 1Pd/AC sorbent. That is because the deactivation of 1Pd5Fe/AC sorbent could be suppressed by abundant Fe_2O_3 on the surface of the fresh 1Pd5Fe/AC sorbent. Fe_2O_3 can react with H_2S to produce elemental sulfur. That can alleviate the formation of PdS due to the reaction between PdO and H_2S. Therefore, the addition of Fe can minimize the deactivation reaction of 1Pd5Fe/AC sorbent during the Hg^0 removal.

Based upon the above discussion, two methods can be proposed to reduce the deactivation of sorbents. The first one is to add some component (such as Fe_2O_3), which can react with H_2S and hence safeguard Pd which helps improve the Hg^0 removal efficiency. The second method is to lower the relative amount of PdO on the surface of sorbents. According to our previous work, When γ-Al_2O_3 was used as a support, PdO was the main component on the surface of both Pd/γ-Al_2O_3 sorbent and Pd-Fe/γ-Al_2O_3 sorbent [21]. When activated carbon (AC) was used as a support, Pd^0 was the main component on the surfaces of Pd/AC [23,24] and 1Pd5Fe/AC sorbents used in this work. So AC as support is favor to the formation of Pd^0 while γ-Al_2O_3 as support is favor to the generation of PdO. The reason might be relate to the oxidation–reduction properties of the supports during the high temperature calcination processing.

4. Conclusions

The Hg^0 removal performance of 1Pd5Fe/AC sorbent at different temperatures in the coal-derived fuel gas with H_2S was investigated. The sorbent performed extraordinarily well compared to the1Pd/AC sorbent at relatively high temperatures (about 200 °C). The results indicated that Fe_2O_3 can react with H_2S resulting in

minimizing the toxic effect of Pd (due to its reaction with H_2S) and enhancing the Hg^0 removal ability of 1Pd5Fe/AC. It can be concluded that the Hg^0 removal active components of the 1Pd5Fe/AC sorbent were elemental Pd and Fe_2O_3. The elemental mercury can be removed by forming Pd–Hg amalgam and HgS. In addition, the reduced atmospheres (H_2 and CO) can enhance the mercury removal efficiency. The mercury removal efficiency improved after a few cycles which can make 1Pd5Fe/AC sorbent a possible candidate for Hg^0 Control at elevated temperatures.

Acknowledgements

This work was supported by National Natural Science Foundation of China (21276170 and 11405256) the Fund Program for the Scientific Activities of Selected Returned Overseas Professionals in Shanxi Province, State Key Laboratory of Coal Combustion and Shanghai Municipal Natural Science Foundation (13ZR1447800). The XAS work was performed at the Shanghai Synchrotron Radiation Facility (SSRF), China and the Canadian Light Source, Canada. The authors also thank the SSRF and CLS staff for the technical support they provided.

References

[1] Xie J, Qu Z, Yan N, Yang S, Chen W, Hu L, et al. Novel regenerable sorbent based on Zr–Mn binary metal oxides for flue gas mercury retention and recovery. J Hazard Mater 2013;261:206–13.
[2] Rodríguez-Pérez J, López-Antón MA, Díaz-Somoano M, García R, Martínez-Tarazona MR. Regenerable sorbents for mercury capture in simulated coal combustion flue gas. J Hazard Mater 2013;260:869–77.
[3] Olson E, Miller S, Sharma R, Dunham G, Benson S. Catalytic effects of carbon sorbents for mercury capture. J Hazard Mater 2000;74:61–79.
[4] Pavlish JH, Sondreal EA, Mann MD, Olson ES, Galbreath KC, Laudal DL, et al. Status review of mercury control options for coal-fired power plants. Fuel Process Technol 2003;82:89–165.
[5] Lim DH, Wilcox J. Heterogeneous mercury oxidation on Au(111) from first principles. Environ Sci Technol 2013;47:8515–22.
[6] Lu Dennis Y, Granatstein DL, Rose Donald J. Study of mercury speciation from simulated coal gasification. Ind Eng Chem Res 2004;43:5400–4.
[7] Poulston S, Hyde TI, Hamilton H, Mathon O, Prestipino C, Sankar G, et al. EXAFS and XRD characterization of palladium sorbents for high temperature mercury capture from fuel gas. Phys Chem Chem Phys 2010;12:484–91.
[8] Spörl R, Belo L, Shah K, Stanger R, Giniyatullin R, Maier J, et al. Mercury emissions and removal by ash in coal-fired oxy-fuel combustion. Energy Fuels 2014;28:123–35.
[9] Spörl R, Maier J, Belo L, Shah K, Stanger R, Wall T, et al. Mercury and SO_3 emissions in oxy-fuel combustion. Energy Procedia 2014;63:386–402.
[10] Stanger R, Ting T, Spero C, Wall T. Oxyfuel derived CO_2 compression experiments with NOx, SOx and mercury removal – experiments involving compression of slip-streams from the Callide Oxyfuel Project (COP). Int J Greenh Gas Control 2015;41:50–9.
[11] Gu Y, Zhang Y, Lin J, Zhang Z, Xu H, Norris P, et al. Homogeneous mercury oxidation with bromine species released from HBr-modified fly ash. Fuel 2016;169:58–67.
[12] Yang J, Zhao Y, Chang L, Zhang J, Zheng C. Mercury adsorption and oxidation over cobalt oxide loaded magnetospheres catalyst from fly ash in oxyfuel combustion flue gas. Environ Sci Technol 2015;49:8210–8.
[13] Zhao Y, Zhang J, Liu J, Diaz-Somoano M, Martinez-Tarazona MR, Zheng C. Study on mechanism of mercury oxidation by fly ash from coal combustion. Chin Sci Bull 2010;55:163–7.
[14] Karatza D, Lancia A, Musmarra D, Pepe F, Volpicelli G. Removal of mercuric chloride from flue gas by sulfur impregnated activated carbon. Hazard Waste Hazard Mater 1996;13:95–105.
[15] Karatza D, Lancia A, Prisciandaro M, Musmarra D, Mazziotti di Celso G. Influence of oxygen on adsorption of elemental mercury vapors onto activated carbon. Fuel 2013;111:485–91.
[16] Karatza D, Prisciandaro M, Lancia A, Musmarra D. Silver impregnated carbon for adsorption and desorption of elemental mercury vapors. J Environ Sci 2011;23:1578–84.
[17] Lee SJ, Seo Y-C, Jurng J, Lee TG. Removal of gas-phase elemental mercury by iodine- and chlorine-impregnated activated carbons. Atmos Environ 2004;38:4887–93.
[18] Tan Z, Su S, Qiu J, Kong F, Wang Z, Hao F, et al. Preparation and characterization of Fe_2O_3–SiO_2 composite and its effect on elemental mercury removal. Chem Eng J 2012;195–196:218–25.
[19] Hou W, Zhou J, Qi P, Gao X, Luo Z. Effect of H_2S/HCl on the removal of elemental mercury in syngas over CeO_2–TiO_2. Chem Eng J 2014;241:131–7.
[20] Jain A, Seyed-Reihani SA, Fischer CC, Couling DJ, Ceder G, Green WH. Ab initio screening of metal sorbents for elemental mercury capture in syngas streams. Chem Eng Sci 2010;65:3025–33.
[21] Han L, Lv X, Wang J, Chang L. Palladium–iron bimetal sorbents for simultaneous capture of hydrogen sulfide and mercury from simulated syngas. Energy Fuels 2012;26:1638–44.
[22] Wang J, Zhang Y, Han L, Chang L, Bao W. Simultaneous removal of hydrogen sulfide and mercury from simulated syngas by iron-based sorbents. Fuel 2013;103:73–9.
[23] Li D, Han J, Han L, Wang J, Chang L. Mid-temperature capture mercury in coal derived fuel gas over Pd/AC sorbents. J Environ Sci 2014;26:1497–504.
[24] Yue C, Wang J, Han L, Chang L, Hu Y, Wang H. Effects of pretreatment of Pd/AC sorbents on the removal of Hg^0 from coal derived fuel gas. Fuel Process Technol 2015;135:125–32.
[25] Wu S, Azharuddin M, Sasaoka E. Characteristics of the removal of mercury vapor in coal derived fuel gas over iron oxide sorbents. Fuel 2006;85:213–8.
[26] Ozaki M, Uddin MA, Sasaoka E, Wu S. Temperature programmed decomposition desorption of the mercury species over spent iron-based sorbents for mercury removal from coal derived fuel gas. Fuel 2008;87:3610–5.
[27] Wu S, Oya N, Ozaki M, Kawakami J, Uddin MA, Sasaoka E. Development of iron oxide sorbents for Hg^0 removal from coal derived fuel gas: sulfidation characteristics of iron oxide sorbents and activity for COS formation during Hg^0 removal. Fuel 2007;86:2857–63.
[28] Wu S, Ozaki M, Uddin MA, Sasaoka E. Development of iron-based sorbents for Hg^0 removal from coal derived fuel gas: effect of hydrogen chloride. Fuel 2008;87:467–74.
[29] Tao L, Guo X, Zheng C. Density functional study of Hg adsorption mechanisms on α-Fe_2O_3 with H_2S. Proc Combust Inst 2013;34:2803–10.
[30] Liu T, Xue L, Guo X, Zheng C-G. DFT study of mercury adsorption on α-Fe_2O_3 surface: role of oxygen. Fuel 2014;115:179–85.
[31] Xue L, Liu T, Guo X, Zheng C. Hg oxidation reaction mechanism on Fe_2O_3 with H_2S: comparison between theory and experiments. Proc Combust Inst 2015;35:2867–74.
[32] Hou W, Zhou J, Zhang Y, Gao X, Luo Z, Cen K. Effect of H_2S on elemental mercury removal in coal gas by Fe_2O_3. P Chin Soc Electr Eng 2013;33:92–8 [in Chinese].
[33] Meng J, Yu Z, Li Y, Li Y. PdS-modified CdS/NiS composite as an efficient photocatalyst for H_2 evolution in visible light. Catal Today 2014;225:136–41.
[34] Li G, Shen B, Lu F. The mechanism of sulfur component in pyrolyzed char from waste tire on the elemental mercury removal. Chem Eng J 2015;273:446–54.
[35] Liu T, Xue L, Guo X. Study of Hg^0 removal characteristics on Fe_2O_3 with H_2S. Fuel 2015;160:189–95.
[36] Zhou JS, Qi P, Hou WH, You SL, Gao X, Luo ZY. Elemental mercury removal from syngas by nano-ZnO sorbent. J Fuel Chem Technol 2013;41:1371–7.
[37] Seo MH, Lim EJ, Choi SM, Nam SH, Kim HJ, Kim WB. Synthesis, characterization, and electrocatalytic properties of a polypyrrole-composited Pd/C catalyst. Int J Hydrogen Energy 2011;36:11545–53.
[38] Datye AK, Bravo J, Nelson TR, Atanasova P, Lyubovsky M, Pfefferle L. Catalyst microstructure and methane oxidation reactivity during the Pd ↔ PdO transformation on alumina supports. Appl Catal A: Gen 2000;198:179–96.
[39] Voogt EH, Mens AJM, Gijzeman OLJ, Geus JW. XPS analysis of palladium oxide layers and particles. Surf Sci 1996;350:21–31.
[40] Brun M, Berthet A, Bertolini JC. XPS, AES and Auger parameter of Pd and PdO. J Electron Spectrosc 1999;104:55–60.
[41] Bhatt R, Bhattacharya S, Basu R, Singh A, Deshpande U, Surger C, et al. Growth of Pd4S, PdS and PdS2 films by controlled sulfurization of sputtered Pd on native oxide of Si. Thin Solid Films 2013;539:41–6.
[42] Romanchenko AS, Mikhlin YL. An XPS study of products formed on pyrite and pyrrhotine by reacting with palladium(II) chloride solutions. J Struct Chem 2015;56:531–7.
[43] Omran M, Fabritius T, Elmahdy AM, Abdel-Khalek NA, El-Aref M, Elmanawi AE-H. XPS and FTIR spectroscopic study on microwave treated high phosphorus iron ore. Appl Surf Sci 2015;345:127–40.
[44] Wang Y-X, Yang J, Chou S-L, Liu HK, Zhang W-x, Zhao D, et al. Uniform yolk-shell iron sulfide-carbon nanospheres for superior sodium-iron sulfide batteries. Nat Commun 2015;6.
[45] Grosvenor AP, Kobe BA, Biesinger MC, McIntyre NS. Investigation of multiplet splitting of Fe 2p XPS spectra and bonding in iron compounds. Surf Interface Anal 2004;36:1564–74.
[46] Liu S, Wang X, Wang K, Lv R, Xu Y. ZnO/ZnS–PdS core/shell nanorods: synthesis, characterization and application for photocatalytic hydrogen production from a glycerol/water solution. Appl Surf Sci 2013;283:732–9.
[47] Chen H, Zhang Z, Yang Z, Yang Q, Li B, Bai Z. Heterogeneous fenton-like catalytic degradation of 2,4-dichlorophenoxyacetic acid in water with FeS. Chem Eng J 2015;273:481–9.
[48] Fleet ME. XANES spectroscopy of sulfur in earth materials. Can Mineral 2005;43:1811–38.
[49] Huggins FE, Huffman GP, Dunham GE, Senior CL. XAFS examination of mercury sorption on three activated carbons. Energy Fuels 1999;13:114–21.
[50] Poulston S, Granite EJ, Pennline HW, Myers CR, Stanko DP, Hamilton H, et al. Metal sorbents for high temperature mercury capture from fuel gas. Fuel 2007;86:2201–3.
[51] Yu TC, Shaw H. The effect of sulfur poisoning on methane oxidation over palladium supported on γ-alumina catalysts. Appl Catal B: Environ 1998;18:105–14.